scientific reports



OPEN

Enhancing the dielectric characteristics and DC flashover of epoxy resin composites by surface modification of AgNbO₃ nano particles

Muhammad Zeeshan Khan^{1⊠}, Faroog Aslam^{2⊠} & Faisal Alsaif³

The advancement of industrial technology has led to power modules facing challenges such as elevated temperatures, high voltages, and increased frequencies. The conventional epoxy resin (Ep) fails to satisfy the demands of high voltage and superior insulation. This study involved the synthesis of Ep resin/ AgNbO₃ nanocomposites aimed at addressing insulating flaws. AgNbO₃ was modified using the silane coupling agent KH550. The changes in the molecular chain after incorporating of unmodified and modified AgNbO, were evaluated through FTIR analysis. The SEM results indicate that following modification, AqNbO₂ particles are evenly distributed within the Ep resin matrix, demonstrating a lack of agglomeration. From thermal conductivity result it was found that modification of AgNbO₃ shows an enhancement of thermal conductivity, attributed to the reduction of interfacial phonon scattering and thermal resistance within the Ep resin. Additionally, the dielectric constant and dielectric loss in composites are greatly impacted by the addition of AgNbO₃. According to the DC breakdown strength result, the addition of modified AgNbO₃ enhanced the process and caused deeper traps to form inside the bulk matrix. The distribution of trap energy levels is determined by Thermal Stimulated Depolarization Current (TSDC), which indicates that the incorporation of AgNbO₃ results in an increase in trap energy levels. Furthermore, the incorporation of 1 wt% AgNbO₃ particle into Ep resin has been observed to enhance the energy level of deep traps. After AqNbO₃ was added, DC Flashover in both air and vacuum significantly increased in comparison to pure Ep resin.

Keywords Niobium silver trioxide (AgNbO₃), Thermal stimulated depolarization current (TSDC), Epoxy resin (EP), Trap energy

Dielectric polymer nanocomposites are garnering significant attention for their potential in high voltage applications within the realm of engineering dielectric and electrical insulation^{1–5}. In contrast to traditional scaled polymer composites, polymer nanocomposites demonstrate significant improvements in their properties.

including improved breakdown strength over time⁶, enhanced resistance to partial discharge and decreased dielectric loss and leakage currents⁷. Moreover, particular unforeseen outcomes have been noted in polymer nanocomposites, suggesting that the challenge of heat accumulation is more evident in large voltage capacity integrated devices, leading to a considerable rise in temperature. Solid dielectric insulation failures at high temperatures can cause irreparable material degradation and drastically shorten the operating life of electrical or electronic equipment⁸⁻¹². The impact of space charge accumulation resulting from elevated temperatures becomes increasingly pronounced, potentially modifying the electric field distribution within the material, hastening the degradation of insulation, and ultimately resulting in insulation failure^{13,14}. Therefore, the advancement of power modules requires the creation of a novel material that exhibits remarkable dielectric properties, effectively reduces space charge, and maintains stability at high temperatures.

¹German Institute of Engineering, Chongqing College of Mobile Communication, Chongqing 401520, Hechuan, People's Republic of China. ²Department of Electrical and Electronics Engineering, Changzhou Institute of Technology, Changzhou 213032, Jiangsu, People's Republic of China. ³Department of Electrical Engineering, College of Engineering, King Saud University, Riyadh 11421, Saudi Arabia. [™]email: ; farooq@czust.edu.cn

EP, a widely used thermosetting polymer, is extensively applied in electronic packaging insulation because of its exceptional insulation properties, processing simplicity, and cost efficiency¹⁵. Nonetheless, the accumulation of space charge and the reduction in electrical performance at higher temperatures limit the further application of Ep. Nanofillers modify traps within the bulk, leading to changes in charge transport characteristics, such as carrier mobility and conductivity. The alterations affect the arrangement of space charges and the electric field in a polymeric material, resulting in a decrease in the energy gain of free carriers, thereby improving the dielectric breakdown performance. Prior investigations suggest that the addition of inorganic fillers such as BN, SiO₂, MgO, AlN, and Al₂O₃ at appropriate filling ratios into Ep can reduce space charge accumulation and enhance breakdown strength^{16–18}. This occurs because inorganic fillers can limit the mobility of molecular chains and the movement of charge carriers^{19,20}. Nonetheless, the interference in charge transport caused by the filler results in the accumulation of a significant amount of net charge on the surface of disc spacers when subjected to prolonged exposure to a DC electric field.

Surface modifiers are categorized into two main types: inorganic modifiers and organic modifiers. Modification of the surface of inorganic fillers can enhance their dispersion and compatibility with polymer matrices are critical factors in material performance. The inorganic modifier reduces the agglomeration in dielectric constant between the inorganic filler and the polymer matrix, while minimally impacting the compatibility between the filler and the matrix. Organic modification, in contrast to inorganic modification, can improve the compatibility between the two phases and enhance the dispersion of inorganic fillers within the polymer.

The enhancement in interfacial compatibility and dispersion results in increased breakdown field strength and polarization strength of the composite material. The composite material exhibits enhanced dielectric properties and improved energy storage performance. Recent investigations indicate that altering the surface of inorganic particles, such as through hydroxylation, the use of coupling agents, surfactants, phosphoric acid and various organic molecules, can greatly improve the dispersion of inorganic fillers within polymers^{21,22}. This modification has the potential to enhance the compatibility between the two materials and contribute to an increase in the breakdown field strength, ultimately leading to improved energy storage density. Significant improvements in dielectric polymer nanocomposites have frequently been anticipated in research studies and reviews, grounded in the existing body of knowledge. However, there are instances where the anticipated benefits do not materialize. In other words, not all dielectric polymer nanocomposites exhibit performance characteristics consistent with those predicted in the existing literature²⁵. The main factors identified are poor dispersion of the nanoparticles and weak interfacial bonding with the polymer, usually due to unsuitable processing techniques.

Zhang et al.²⁶ examined the influence of doped ZnO nanoparticles on the flashover voltage of epoxy resins at 77 K, revealing that nanoparticle modulation of trap distribution at cryogenic temperatures could elevate the flashover voltage. Lee et al.²⁷ assessed the impacts of nano ${\rm TiO_2}$ and nano ${\rm Al_2O_3}$ on the surface insulation characteristics of epoxy resins in a 77 K environment, concluding that nano ${\rm Al_2O_3}$ was superior to nano ${\rm TiO_2}$ in enhancing both partial discharge inception voltage (PDIV) and flashover voltage. Tu et al.²⁸ investigated the effect of vacuum on flashover within the temperature range of 300–20 K, determining that flashover under lower vacuum conditions is predominantly influenced by gas discharge.

Still, determining the optimal organic filler to enhance the flashover, breakdown and thermal properties of Ep presents a novel challenge. A case study was carried out to explore the previously mentioned question and to examine epoxy/AgNbO₃ nanocomposites, which serve as the closest representation of ideal dielectric polymer nanocomposites. Three significant advantages of these nanocomposites are emphasized for analyzing structure-property relationships. Initially, the individual AgNbO₃ molecules can be significantly treated with silane coupling agent. Furthermore, the terminal groups of AgNbO₃ have the capacity to interact with the polymer matrix between its two phases, resulting to the occurrence of a covalent bonding interface. Ultimately, the treated AgNbO₃ molecules exhibit solubility in solvents at the molecular level, facilitating a more straightforward and manageable approach to composite processing when compared to other particulate composites. The presence of these three advantages indicates that modified AgNbO₃ can be integrated into polymers at the molecular scale, enabling the full realization of the nano-effect. This implies that modifications in the polymer superstructure and chain dynamics at the interfacial regions are achievable, potentially resulting in notable changes in the composite properties.

In this study, Ep resin reinforced with AgNbO₃ at various concentrations was prepared. AgNbO₃ underwent treatment with the silane coupling agent KH550 to restrict agglomeration. Moreover, chemical bonding, thermal conductivity, and DC breakdown strength were investigated. The distribution of traps was determined utilizing MATLAB. Furthermore, DC flashover in both air and vacuum has been analyzed.

Material and experimental method Materials

The epoxy resin used is Phoenix brand bisphenol A-type E-51 epoxy resin (Nantong Xingchen Synthetic Materials Co., Ltd.), the curing agent is methyl tetrahydrophthalic anhydride (MTHPA, Jiaxing Dongfang Chemical Plant), and the accelerator is selected using DMP-30 (Aladdin Industrial Corporation).

Preparation of AgNbO₃ particles

AgNbO $_3$ was synthesized by separately dissolving AgNO $_3$, Persulfate (PS) oxidant from Nanjing Reagent Co., Ltd, and Nb $_2$ O $_5$ from Sinopharm Chemical Reagent Co., Ltd in acetic acid. The resulting solutions were subsequently combined and adjusted to a pH of 2–3 with ammonia to achieve the desired solution. Ethylene glycol was incorporated into the solution, and the precipitate was subsequently separated. Particles of AgNbO $_3$ were synthesized through the calcination of the precursor at a temperature of 800 °C for a duration of 6 h.

Treatment of AgNbO₃ particle

AgNbO₃ particles were combined with anhydrous ethanol and deionized water. The mixture was agitated to facilitate the bonding of hydroxyl groups on the surface of AgNbO₃ particles, leading to the formation of AgNbO₃@OH particles. Subsequently, the silane coupling agent KH550 was introduced to anhydrous ethanol and stirred for 30 min. Following this, AgNbO3@OH particles were incorporated into the mixture at volume ratio of volume ratio of 1:1:18 and stirred for 8 h at 400 rpm. The modified AgNbO₃ particles were then dried at 60 °C for 12 h.

Sample preparation

The materials selected for this experiment included bisphenol A epoxy (EP) resin and an acid anhydride curing agent, specifically methyl hexahydrophthalic anhydride, both of which are commonly used in the field of electrical engineering. To facilitate the curing process, dimethyl benzyl amine was employed as an accelerating agent, effectively lowering the curing temperature of the epoxy resin and reducing the overall curing time. The complete procedure for sample preparation is depicted in Fig. 1 initially, the EP resin was transferred into a beaker, after which acetone was carefully introduced in appropriate proportions to achieve proper dilution.

Subsequently, the required quantities of nanoparticles were added to the mixture. The $AgNbO_3$ nanoparticles were pre-dispersed by stirring the mixture for a duration of 30 min using a high-shear mechanical mixer operating at a speed of 1500 rpm and maintained at a temperature of 60 °C. Subsequently, the nanofillers were subjected to further dispersion for 30 min using an ultrasonic device. Upon confirming the total evaporation of acetone from the beaker, precise proportions of curing and accelerating agents were added to the mixture (epoxy resin: curing agent: accelerating agent weight ratio = 100:90:2). The mixture was then vigorously stirred and degassed in a vacuum for about 30 min at a temperature of 50 °C. The liquid was subsequently put into a plate mold and underwent oven curing at 90 °C for 2 h and 110 °C for next 2 h. The modified and unmodified $AgNbO_3$ / Ep resin composites with different concentrations were obtained after being fully cooled in air following the curing process. Afterward, the samples were washed with ethanol to remove any surface residues and then placed in a chamber at 40 °C for one day to ensure complete drying. The epoxy composite specimens prepared for dielectric characterization had a diameter of 100 mm and a thickness of 0.5 mm.

Experimentation details

Utilizing FTIR on an Alpha instrument provided by Bruker, the chemical changes were examined. FTIR spectra were acquired at a resolution of $4.0~\rm cm^{-1}$ over a wavelength range of 400– $4000~\rm cm^{-1}$. XPS analysis was conducted using ESCALAB 250XI (Thermo Fisher Scientific Inc., Waltham, MA, USA), utilising monochromatic Al K α X-ray radiation (1486.6 eV). The crystalline structure was identified using X-ray diffraction (XRD, X'Pert Pro Philips, Dandong, China).

In order to investigate the morphology of the Ep resin/AgNbO $_3$ nanocomposites, scanning electron microscopy (SEM, Zeiss LEO $_2$, DSM 982) was used. Thermal conductivity was measured using the DRL-III thermal conductivity device from Xiangtan Equipment Company and the planar heat flow method. The temperature range that was examined was between 15 and 165 °C. A digital electrometer (Advantest R8252) was used to measure the thermally stimulated depolarization current (TSDC). Using equipment from NoVo Control Technologies, Montabaur, Germany, the dielectric constant and dielectric loss were measured at frequencies between 10^{-1} and 10^{6} Hz. To perform the DC breakdown, an electrode arrangement with a finger-like shape and a diameter of 25 mm was used. Additionally, until breakdown occurred, a high-voltage electrode was exposed to a direct current voltage application at a rapid rate of around 0.5 kV s⁻¹. The thermally induced release of polarization charges in EP/AgNbO $_3$ composites is investigated using the TSDC analysis approach. All samples were polarized for 30 min at 90 °C and 333 V/mm prior to cooling with N2 gas. After the samples were depolarized by a linear heating process from 20 to 160 °C at a rate of 3 °C per minute, the depolarization current was measured using an electrometer (Keithley 6517B).

For DC flashover in air both electrodes consist of stainless steel, featuring edges rounded to a 25 mm radius, while sockets for banana plugs are positioned at the rear of each electrode as shown in Fig. 2. Moreover, the

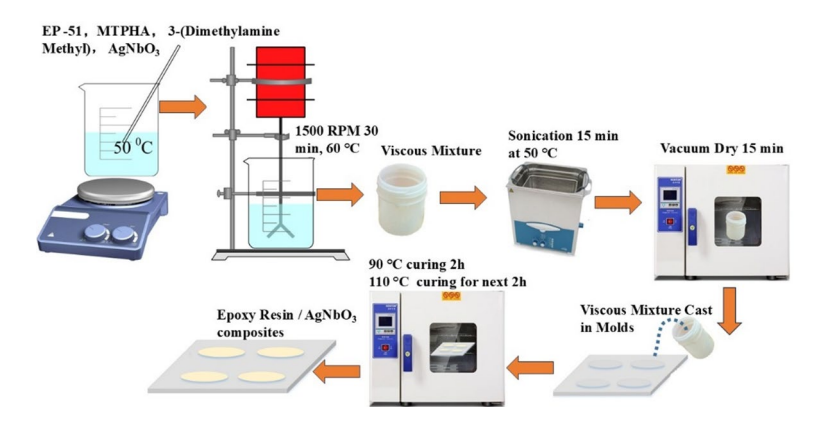


Fig. 1. Synthesis of Ep resin / AgNbO₃ composites.

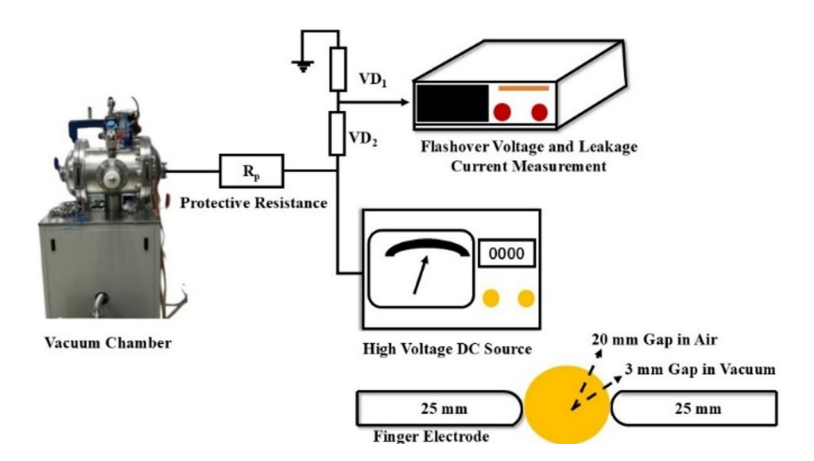


Fig. 2. Experimental setup for DC surface flashover measurement in air and vacuum.

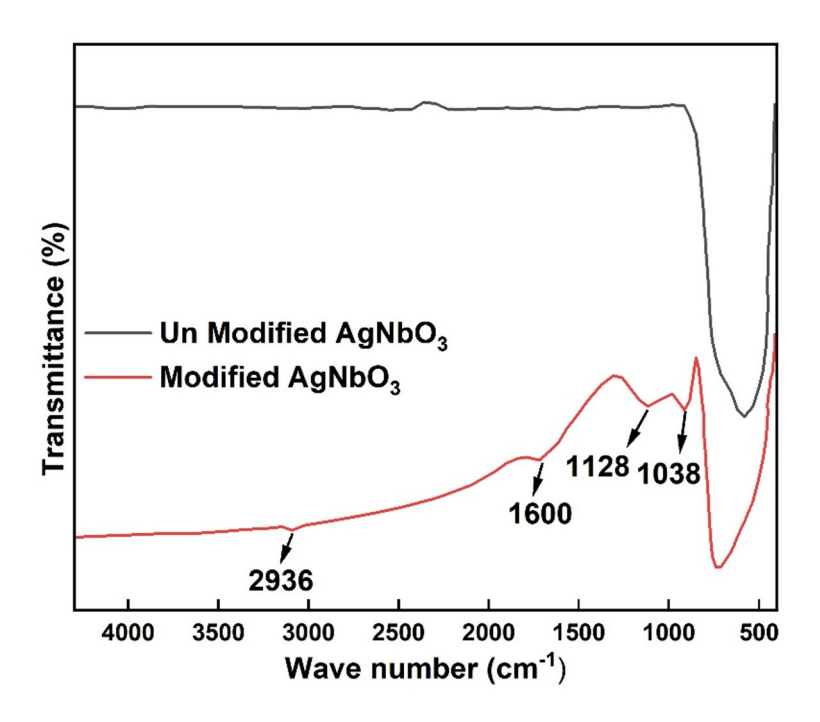


Fig. 3. Fourier-transform infrared spectra obtained for AgNbO₃ before and after modification.

sample holder's base is constructed from Teflon. The distance between the electrodes can be modified; however, for the purposes of this experiment, it was established at an optimal 20 mm. Samples of epoxy resin with a thickness of 0.5 mm were utilized, positioned between the electrode pair and the Teflon base.

The samples were exposed to a progressively increasing voltage of $0.2\,\mathrm{kV/s}$ until flashover occurred, at which point the flashover voltage was documented. This test was conducted multiple times with different epoxy samples at various concentrations of $\mathrm{AgNbO_3}$. Observations indicate that following several flashover events, pitting marks were evident on the edges of both stainless-steel electrodes. Consequently, the electrodes underwent repolishing after every five flashovers to eliminate the pitting signs, ensuring more consistent results. Additionally, for the vacuum flashover test, the electrode gap is established at 3 mm, adhering to the limitations imposed by the switching overvoltage tolerance of the experimental setup. For each sample, twenty flashover measurements were conducted, and the Weibull model was employed to ascertain the flashover voltage of the samples.

Result

FTIR spectroscopy

The FTIR spectroscopy results of both unmodified and modified AgNbO₃ are presented in Fig. 3. The absorption band seen at around 2936 cm⁻¹ was ascribed to the -OH groups. The peak at 1600 cm⁻¹ corresponds to the absorption vibration of -NH₂, and the peak at 1130 cm⁻¹ signifies the stretching vibration associated with the C-N bond. The peak at 1038 cm⁻¹, absent in unmodified AgNbO₃, corresponds to the characteristic stretching

vibration of the Si-O bond formed by the chemical reaction between AgNbO₃ particles and KH550²⁹. The absorption peak indicates that the AgNbO₃ particles have been effectively modified.

XRD analysis

Figure 4 illustrates the X-ray diffraction (XRD) pattern of AgNbO₃ particles before and after modification. It was observed that the XRD peaks of AgNbO₃ particles remain the same before and after surface modification. The result indicates that the particle structure is unaffected by the surface modification process involving silane coupling agents. Consequently, the surface modification technique does not affect the particle structure.

XPS analysis

X-ray photoelectron spectroscopy was employed to confirm the deposition of KH550 on AgNbO₃ powder. The C1 peak may be divided into five distinct summits. Figure 5a demonstrates that the C-Si bond has a binding energy of 283.8 eV, the C-C bond has a binding energy of 284.9 eV, and the C-N link has a binding energy of 286 eV. This confirms that the silane coupling agent KH550 has been successfully grafted onto the surface of AgNbO3. The O1 peak consists of three overlapping sub-peaks, as seen in Fig. 5b. The Ag-O bond has a binding energy of 529.3 eV, whereas the Si-O bond displays a binding energy of 532 eV, attributed to the interaction between AgNbO₃ and the silane coupling agent KH550. The -OH group at 531.45 eV is the source of hydroxyl radicals in the silane coupling agent KH550. Figure 5c demonstrates that the Si 2p peak may be deconvoluted into two separate peaks. The Si-OH bond has a binding energy of 102.5 eV, while the Si-C bond has a binding energy of 101.88 eV. The values originate from the silane coupling agent KH550³⁰. The alterations in the surface of AgNbO₃ indicated that the silane coupling agent KH550 was successfully applied to the AgNbO₃ powder.

SEM analysis

Figure 6a-c shows the SEM images illustrating the surface morphology of the EP resin/AgNbO₃ nanocomposite at a 5 wt% concentration. At this concentration, the unmodified AgNbO₃ exhibits considerable aggregation, with particle sizes reaching approximately 540 nm, due to numerous interfaces forming between the unmodified AgNbO₃ and the epoxy resin matrix as shown in Fig. 6b. In contrast, Fig. 6c reveals a uniform distribution of modified AgNbO₃ nanoparticles within the EP matrix, indicating minimal agglomeration. The dispersion of the modified AgNbO₃ particles within the epoxy resin was notably enhanced, largely due to the replacement of several hydroxyl groups on the AgNbO₃ surface with a silane coupling agent. This modification reduced the chemical bonding potential with hydroxyl groups, allowing the AgNbO₃ to remain as individual particles, thereby promoting better dispersion within the EP resin.

Thermal conductivity

Figure 7 shows how adding AgNbO₃ at various concentrations and temperatures causes variations in the thermal conductivity of Ep resin composites. The heat conductivity of Ep composites is significantly increased by the addition of AgNbO₃. The enhancement is exactly proportional to the concentration of AgNbO₃ in the Ep resin. This phenomenon can be elucidated by the following reasons: Amorphous polymers encompass both pure Ep resin and its composites. Phonons, which facilitate quantum vibrations, are essential for heat conduction in amorphous polymers. Phonon dispersion significantly influences thermal resistance and heat conduction

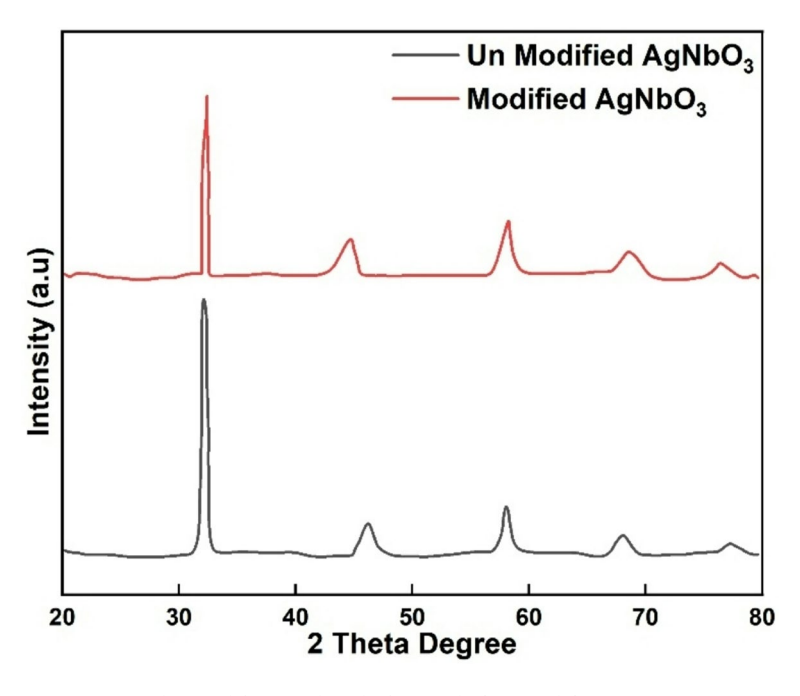


Fig. 4. XRD obtained for AgNbO₂ before and after modification.

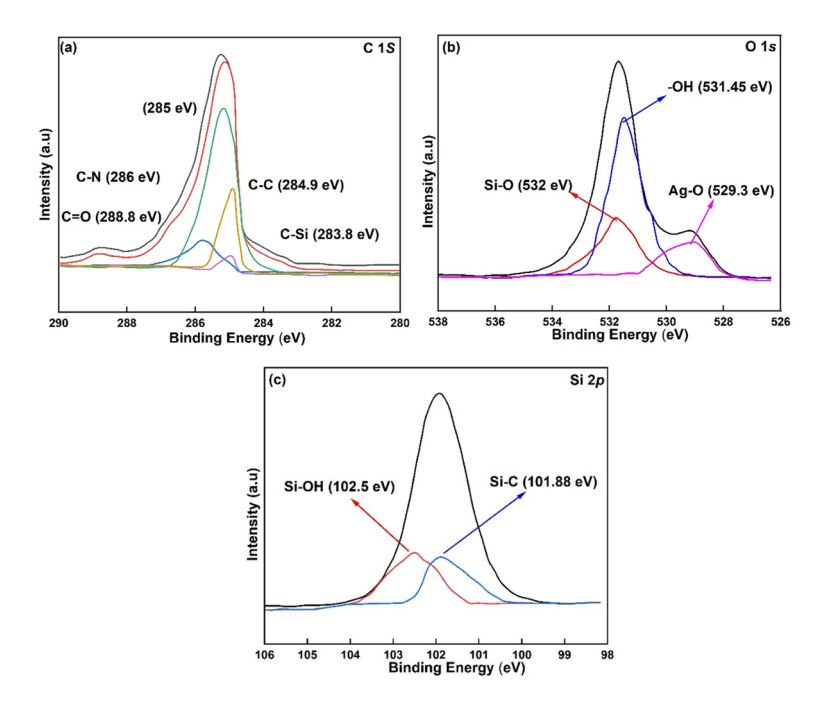


Fig. 5. XPS Analysis of Modified AgNbO₃, (a) C 1s spectrum, (b) O 1s spectrum, (c) Si 2p spectrum.

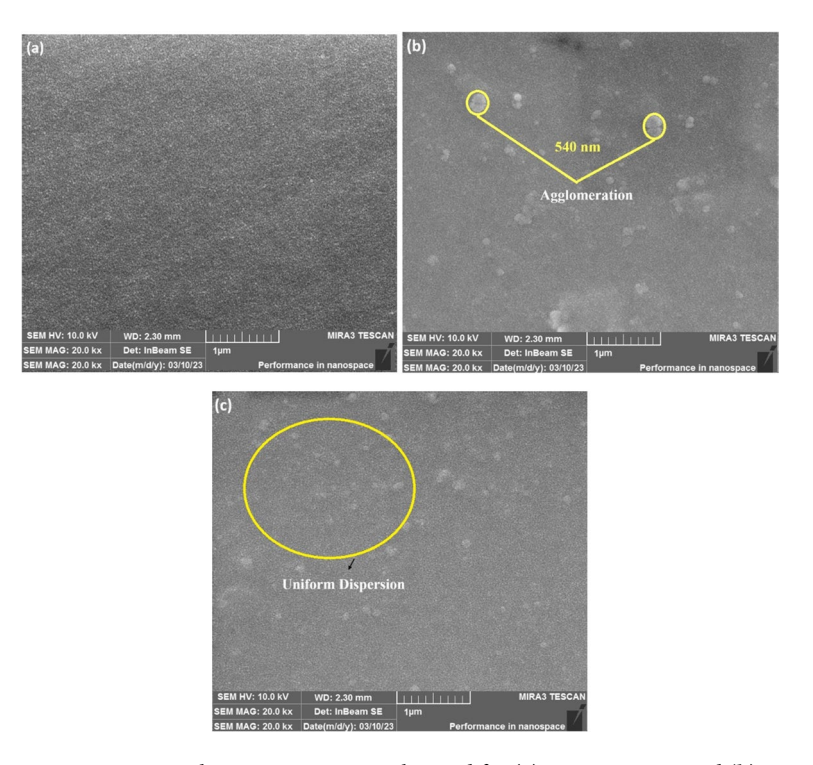


Fig. 6. Scanning electron microscopy obtained for **(a)** Pure Ep Resin and **(b)** Un Modified, **(c)** Modified obtained at 5 wt% of Ep resin / AgNbO₃ composites.

efficiency, especially at low temperatures. The molecular chains of pure Ep resin randomly intertwine due to its low crystalline structure, leading to the notable occurrence of phonon scattering. As a result, pure Ep resin demonstrates minimal thermal conductivity.

It was also observed that the thermal conductivity of Ep resin increases after incorporation of AgNbO₃ that acts as a bond between the molecular chains of Ep, strengthening the heat transfer between these chains and thereby enhancing the thermal conduction efficacy of Ep composites. It was also seen that after modification of

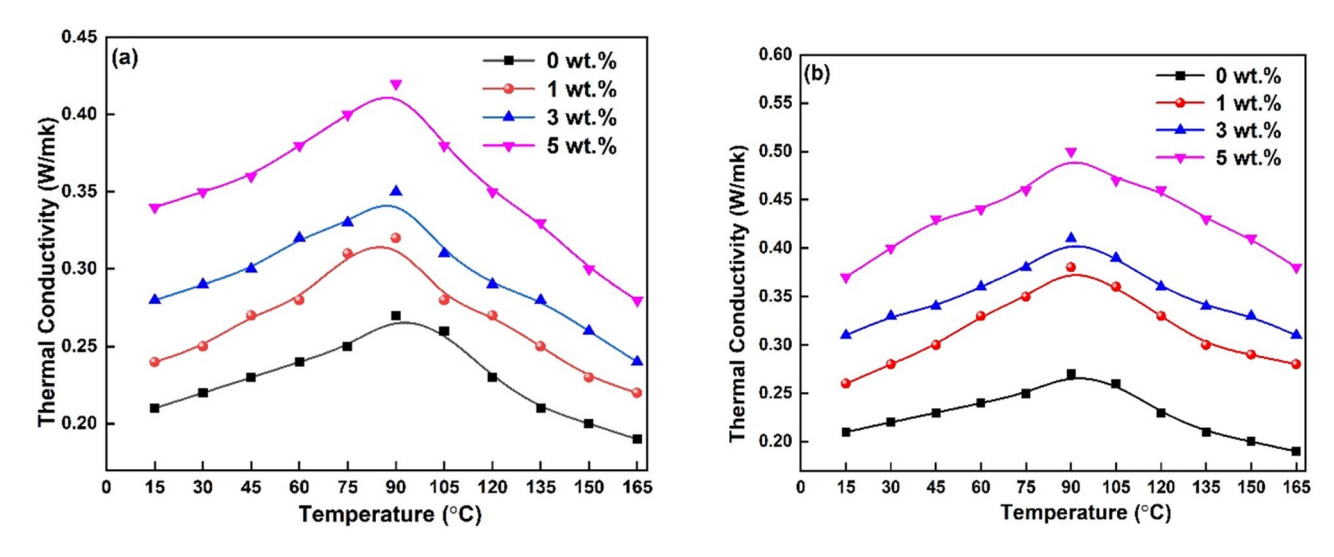


Fig. 7. Thermal conductivity obtained for AgNbO₃ (a) Un modified, (b) Modified obtained at various concentration of Ep resin/ AgNbO₃ composites.

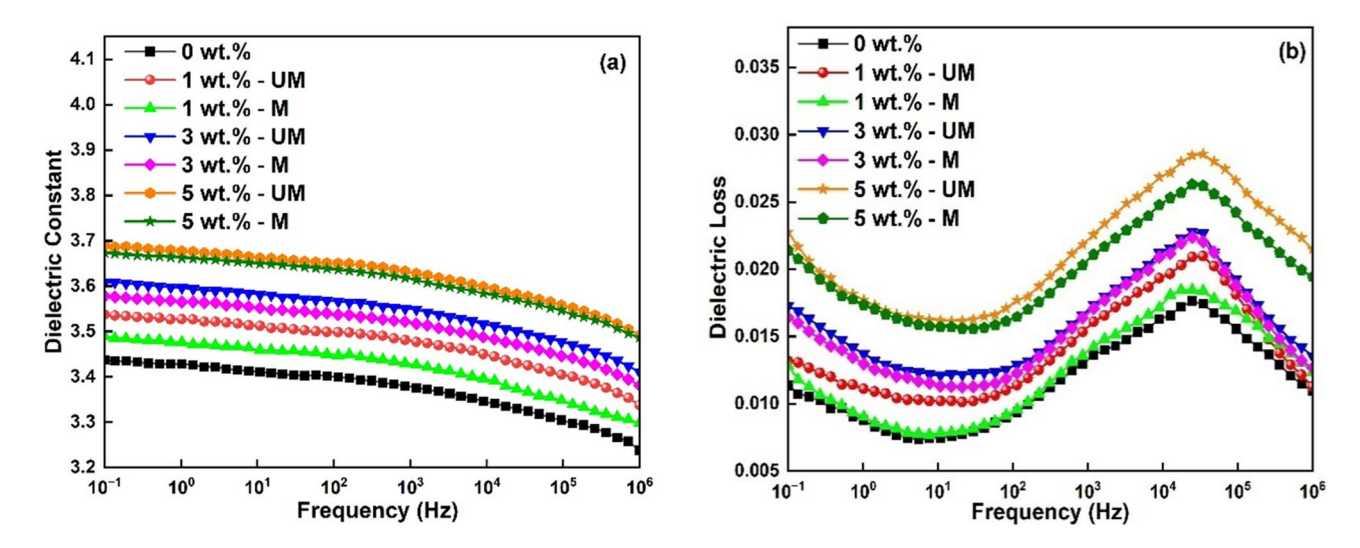


Fig. 8. (a) Dielectric Constant, (b) Dielectric Loss obtained for AgNbO₃ of Un modified and Modified obtained at various concentration of Ep resin/ AgNbO₃ composites.

 ${\rm AgNbO_3}$ shows enhanced thermal conductivity due to the reduction of the interfacial phonon scattering and thermal resistance inside the Ep resin.

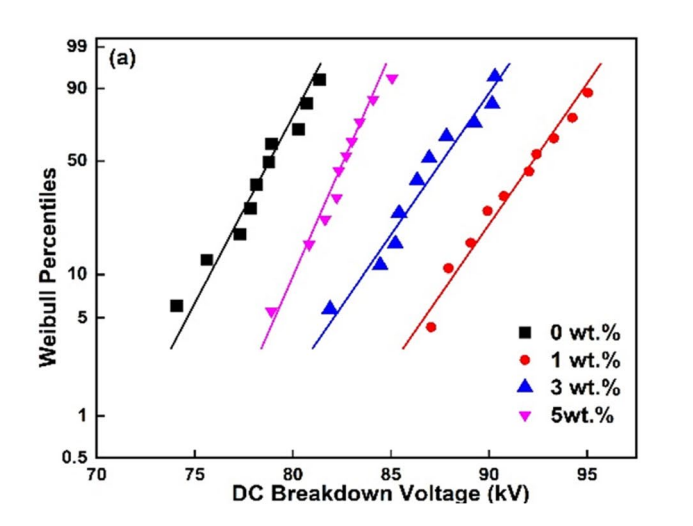
Furthermore, it was observed that the thermal conductivity reduces as the temperature rises, which is attributed to the thermal expansion of the composite. As temperature rises, the volume of the composite expands, resulting in an increased gap between the resin and filler. This expansion obstructs phonon transition, ultimately causing a reduction in the thermal conductivity of the composite. The results obtained at higher temperatures aligned with the findings of Ying et al.³¹ on the impact of thermal conductivity in EP resin by incorporating carbon fiber and boron nitride at different filler concentrations.

Dielectric spectroscopy

Figure 8 demonstrates the differences in dielectric constant and dielectric loss for the Ep resin incorporating both unmodified and modified $AgNbO_3$ at different concentrations. Measurements were carried out at ambient temperature (20 ± 5 °C). The findings demonstrate that the addition of $AgNbO_3$ doping resulted in an enhancement of both the dielectric constant and dielectric loss of the composites in comparison to pure Ep resin. This phenomenon can be explained by the following factors: $AgNbO_3$ is recognized as a ferroelectric material that demonstrates a significantly higher dielectric constant and dielectric loss compared to pure epoxy resin. The rise in dielectric loss can also be linked to enhanced interfacial polarization and localized charge buildup resulting from the presence of nanoparticles and the interfacial zones established between the filler and the matrix. Similar findings are also observed in epoxy combined with various fillers, including Al_2O_3 and Al_2O_3 .

Composite	Dielectric constant at 0.1 Hz	References
EP/γ-Al ₂ O ₃ nanocomposites	0 wt% = 3.91, 1 wt% = 4.2, 3wt.% = 4.5, 5 wt% = 4.65	36
EP/ Modified SiO ₂ nanocomposites	0 wt% = 3.7, 1 wt% = 3.81, 2.5 wt% = 4, 5 wt% = 4.24	37
EP/ MgO nanocomposites	0 wt% = 4, 1 wt% = 4.5, 3 wt% = 5.1	38
EP/Modified AgNbO ₃ composites	0 wt% = 3.43, 1 wt% = 3.48, 3 wt% = 3.57, 5 wt% = 3.67	This work

Table 1. Dielectric constant of EP resin incorporated with various filler concentration compared with other studies.



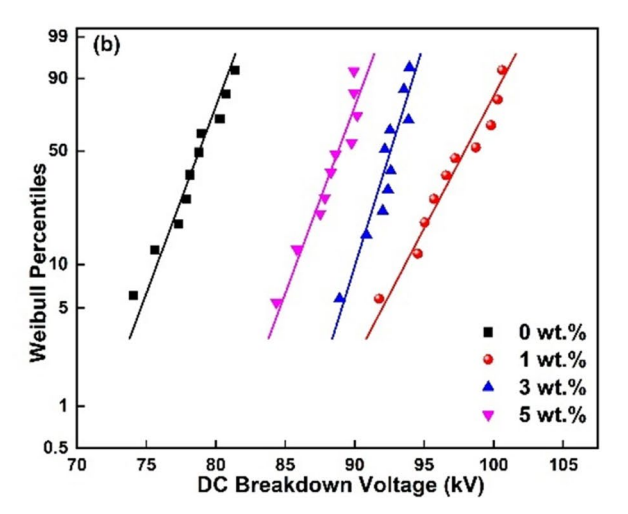


Fig. 9. DC Breakdown strength **(a)** Un-Modified, **(b)** Modified AgNbO₃ obtained at various concentration of Ep resin/ AgNbO₃ composites.

It was observed that the dielectric constant initially increases at lower frequencies and subsequently decreases at higher frequencies. The observed phenomenon can be linked to the prevalence of dipole polarization at lower frequencies. At higher frequencies, the dipoles within the material cannot adequately respond, leading to a diminished level of polarization.

This, in turn, results in a reduction of both the dielectric constant and dielectric loss of the EP resin / AgNbO₃ nanocomposites at elevated frequencies. Additionally, the following parameters may be used to explain the lowered values of the dielectric constant and dielectric loss of the Ep resin with varying concentrations of modified AgNbO₃ at all concentration. By creating covalent bond at the interface, the silane coupling agent (KH550) successfully acted as a barrier between the Ep resin and the modified AgNbO₃. The interaction resulted in a reduction of polarizable hydroxyl groups and limited the mobility of charge carriers on the surfaces of the modified AgNbO₃ particles, thereby enhancing their dispersion in the Ep resin. As a result, these factors led to a reduction in dielectric constant and dielectric loss^{34,35}. Table 1 presents a comparative investigation of the dielectric constant values acquired in our study against those reported in the existing literature. The findings demonstrate a significant reduction in the dielectric constant relative to other studies.

DC breakdown strength

The Weibull distribution of the DC breakdown and flashover voltage data, derived from fitting the measured voltages for each sample, is illustrated in Figs. 9 and 11. The Weibull distribution is commonly utilized in reliability engineering to characterize the occurrence of overall failure attributed to a link within a chain system. The method allows for straightforward inference of distribution parameters through probability values, making it a common choice for assessing the overall lifespan of the system. To facilitate a more intuitive analysis of the flashover voltage of Ep resin composites, the Weibull distribution was employed to process the recorded 10 breakdown Voltages and 20 flashover voltages. The cumulative probability function of the two-parameter Weibull distribution is defined.

$$A = 1 - \exp\left(\frac{b}{c}\right)^{\alpha} \tag{1}$$

	Ep resin/Un modified AgNbO ₃ nanocomposites		Ep resin/ modified AgNbO ₃ nanocomposites	
Sample wt%	a (kV)	β	a (kV)	β
0	78	39	78	39
1	91	59	97	87
3	87	41	92	66
5	82	44	88	42

Table 2. Weibull parameters for DC breakdown strength of ep resin incorporated with Un modified and modified AgNbO₂ at different concentrations.

Concentration wt%	Peak temperature/℃	Trap energy (eV)
0 wt%	98.61	1.94
1 wt%	115.82	2.65
3wt.%	110.59	2.45
5 wt%	102.84	2.25

Table 3. Trap parameter obtained for modified $AgNbO_3$ at various concentration of ep resin/ $AgNbO_3$ composites.

where b denotes a variable that represents the absolute value of the flashover voltage of the sample. A represents the failure probability associated with a voltage level of b, indicating the likelihood of break down and flashover occurring when the sample is subjected to a voltage of b or lower. c denotes the sample scale parameter, indicating the flashover voltage corresponding to a failure probability of 63.2%. α represents the shape parameter and serves as an indicator of the stability of flashover on the sample. The formula for median rank is presented to adjust the failure level, and the expression for the failure level is

$$X = \frac{d - 0.3}{e + 0.4} \times 100\% \tag{2}$$

In this context, d represents the sample number, while e denotes the total number of samples.

Figure 9 depicts the DC breakdown strength of the Ep resin/AgNbO₃ prior to and following modification. Figure 9a; Table 2 illustrates that the breakdown strength under DC current increases as the concentration of AgNbO₃ is elevated. Moreover, a rise in trap energy contributes to the enhancement of the DC breakdown strength in the nanocomposites, with the interaction zone playing a critical role in shaping the trap characteristics of the nano-dielectric²⁰. At a lower AgNbO₃ concentration, particularly at 1 wt%, the distinct interaction zones formed by AgNbO₃ particles lead to an increase in deep trap density, thereby improving the breakdown strength of the nanocomposites. However, when the AgNbO₃ concentration surpasses 1 wt%, the overlapping of contact regions may result in a prolonged electron transport pathway. Upon the application of an electric field, carriers can navigate these conduction pathways more easily, resulting in a decrease in the breakdown strength of the nanocomposites.

A comparable pattern was observed in the research by Chen et al.³⁹, which focused on enhancing the electrical properties of epoxy resin using α -phase Al_2O_3 nanoparticles. It was also found that adding 2 wt% of α -Al₂O₃ improves the DC breakdown strength, which increases the cross-linking density in the interaction zone.

In Fig. 9b, it was noted that the DC breakdown strength increased following the modification of $AgNbO_3$ with a Silane coupling agent, which effectively enhanced the compatibility between the organic and inorganic phases. Consequently, the formation of aggregations of $AgNbO_3$ in Ep resin is relatively challenging due to the steric hindrance effect, while also offering active groups that facilitate the establishment of covalent bonds during the cross-linking reaction. These factors significantly improve the dispersion of $AgNbO_3$ particles in Ep resin, thereby enhancing DC breakdown strength. Moreover, the β of Ep resin incorporated with Modified $AgNbO_3$ as shown in Table 2 exhibits a relatively larger value than that of the unmodified EP Resin $AgNbO_3$ composite, attributable to the uniform dispersion of surface-modified nanofillers resulting in enhanced data.

TSDC analysis

The graph in Fig. 8 shows the thermally stimulated depolarization current curve for Ep resin/AgNbO₃ nanocomposites. The trap energy can be determined using MATLAB by fitting the experimental TSDC values to the designated Eq. $(1)^{40}$, with the trap energy level indicated in Table 3.

$$j(T) = B\left(e^{\left(-\frac{Et}{k_BT}\right)} - \frac{1}{\xi\tau_0} \int_{T_0}^T e^{\left(-\frac{E_T}{k_BT}\right)} dT'\right)$$
(3)

Whereas, j(T) denotes the TSDC current density quantified in Am⁻². The variable B represents a constant, which can also be expressed in Am⁻². The term E_T denotes the activation energy linked to the relaxation process, measured in electron volts (eV). The parameter ϵ represents the heating rate, defined in Ks⁻¹. The relaxation time constant is denoted as $\tau 0$ and is measured in seconds (s). The symbol kB represents the Boltzmann constant, whereas T denotes the temperature in ${}^{\circ}C$.

Figure 10 indicates that the temperature of the TSDC peak increases compare to pure Ep resin, implying that the addition of fillers alters the mobility of charge carriers and can create deep traps. From Table 3 it was observed that the trap energy first increases and then decreases as the concentration of modified AgNbO₃ filler rise. The observed trend of trap energy levels correlates with the findings of Guoqing et al. 41 by integrating nano silica into epoxy resin at varying filler concentrations. The results reveal that the trap energy level initially rises at 1 wt% and subsequently reduce with increasing nano silica concentration.

Furthermore, the incorporation of $AgNbO_3$ into Ep resin leads to the formation of a cross-linking layer, which introduces deep traps capable of capturing electrons. This process hinders electron migration, thereby reducing space charge injection within the sample and enhancing its dielectric properties. Also, at higher filler concentration of $AgNbO_3$ could result in the overlap of interaction regions. The overlap can establish a conductive pathway, potentially leading to a reduction in charge trapping and, consequently, a decrease in trap energy.

DC flashover

The data from Fig. 11a-d; Tables 4 and 5 indicates that the flashover voltage for both air and vacuum initially rise before decreasing at higher concentrations of $AgNbO_3$, specifically at 3 wt% and 5 wt%. The multi-region structure surrounding the nanoparticles indicates that interaction zones have developed within the Ep resin matrix following the incorporation of $AgNbO_3^{42}$.

The interaction zone model, featuring a multi-region structure, is divided into three distinct areas: the bonded region, the transitional region, and the normal region. Among these, the transitional region is characterized by the greatest thickness and is considered the most critical. This interaction zone is treated as an independent phase, separate from the polymer matrix. Within this zone, a new potential barrier is anticipated to form, which interacts with the existing barrier in the matrix, thereby modifying the trap parameters of the nanocomposites. Even a small amount of AgNbO₃ can generate significant, independent interaction zones in the matrix that align with the potential barrier, leading to the formation of deeper traps for the nanoparticles. Some studies have reported that the incorporation of fillers into nanocomposites can substantially increase the depth of these traps, whereas the shallow traps may exhibit only a slight increase or potentially even a reduction⁴³.

Figure 11a-d demonstrated that the presence of deep traps contributes to an increase in surface flashover voltage. With the rise in AgNbO₃ concentration, the charged particles generated during voltage escalation begin to interact with the dielectric surface, resulting in charge accumulation on the surface of the epoxy resin. This surface charge alters the applied electric field, ultimately leading to a reduction in DC flashover voltage. However, the DC flashover performance of the Ep resin/AgNbO₃ nanocomposites in both air and vacuum conditions improved after the surface modification of AgNbO₃. The silane coupling agent (KH550) served as an effective interfacial barrier between the epoxy resin and the modified AgNbO₃, promoting the formation of covalent bonds at the interface. This bonding reduced the number of polarizable hydroxyl groups and restricted charge carrier mobility on the surface of the treated AgNbO₃ particles, which also exhibited improved dispersion within the epoxy matrix. Collectively, these effects contributed to the enhancement of DC flashover voltage in both air

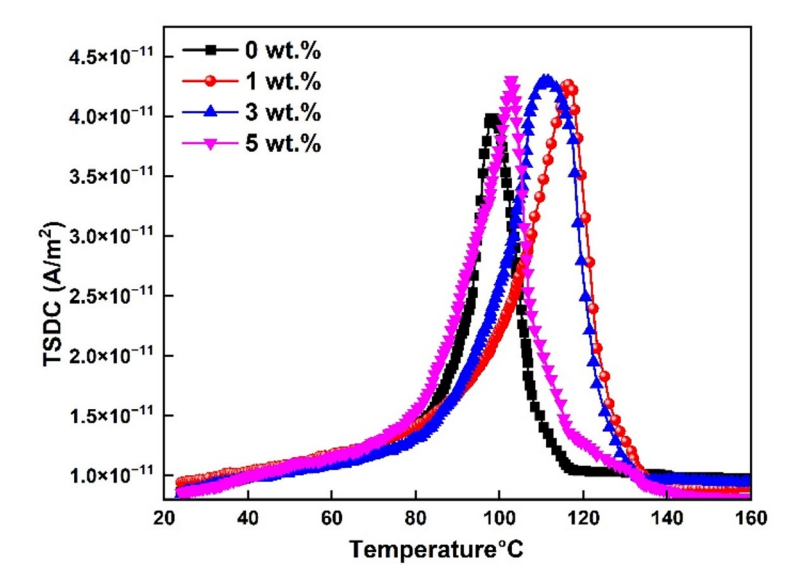


Fig. 10. TSDC spectrum obtained for Modified ${\rm AgNbO_3}$ at various concentration of Ep resin/ ${\rm AgNbO_3}$ composites.

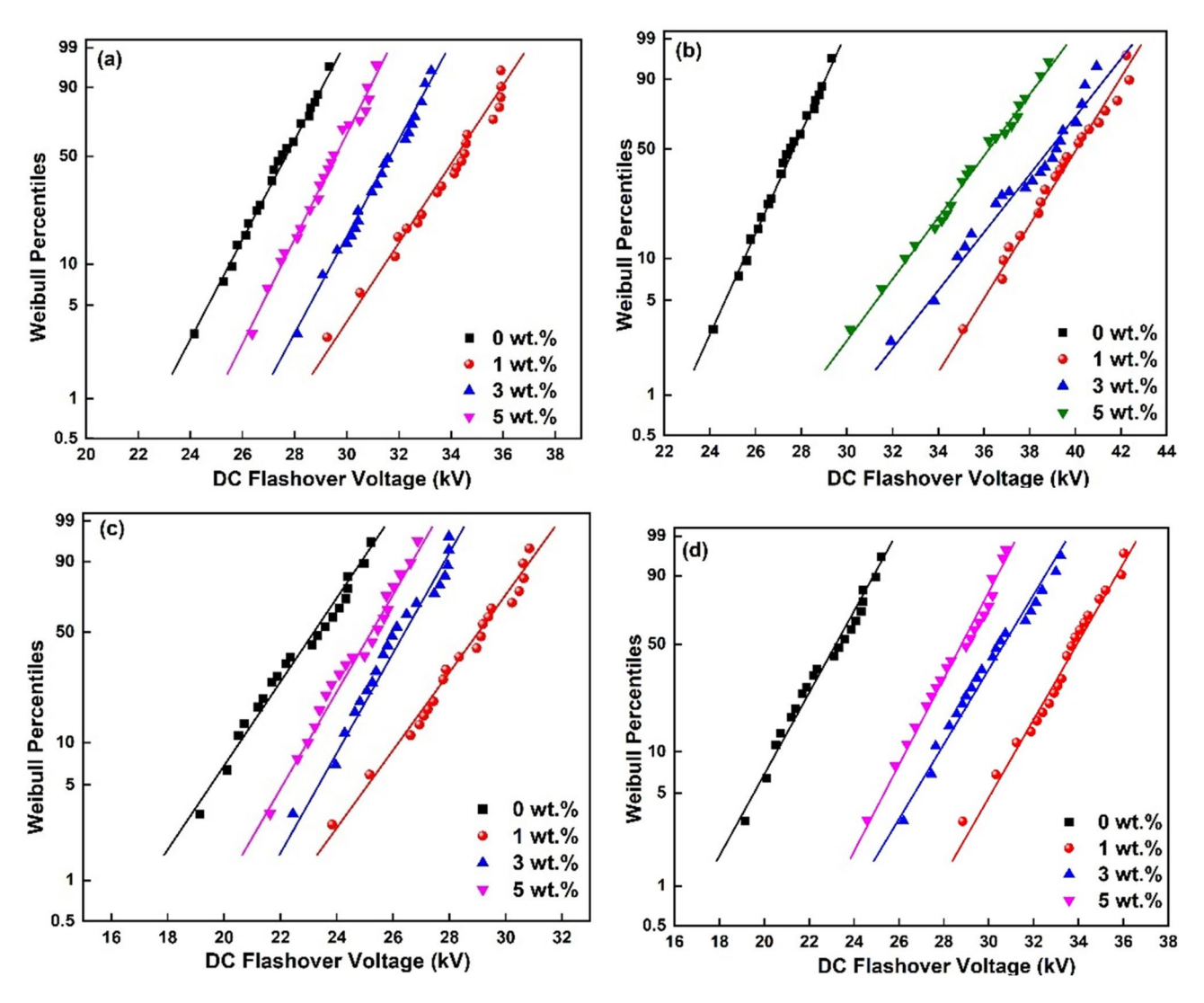


Fig. 11. DC Flashover in air (a) Un-Modified (b) Modified, DC Flashover in Vacuum (c) Un-Modified (d) Modified AgNbO₃ obtained at various concentration of Ep resin/ AgNbO₃ composites.

	Ep resin/Un modified AgNbO ₃ nanocomposites		Ep resin/ modified AgNbO ₃ nanocomposites	
Sample wt%	a (kV)	β	a (kV)	β
0	27	23	27	23
1	34	25	39	27
3	31	21	37	26
5	29	19	35	24

Table 4. Weibull parameters for DC flashover strength of ep resin in air incorporated with Un modified and modified $AgNbO_3$ at different concentrations.

and vacuum environments. A comparable trend has been noted by Yunqi et al. 44 , indicating that the inclusion of modified ${\rm SrTiO_3}$ in epoxy resin significantly contributes to the acceleration of surface charge de-trapping and the reduction of charge accumulation, thereby effectively improving the discharge and surface flashover voltage of the composite.

The incorporation of both unmodified and modified $AgNbO_3$ resulted in a noticeable increase in DC flashover in vacuum, as illustrated in Fig. 11c, d. This phenomenon can be elucidated through the subsequent factors: The onset of primary electrons in vacuum flashover generally takes place at the triple junction point, where the electrode interacts with the Ep resin/ $AgNbO_3$ nanocomposite. The dielectric surface experiences bombardment

	Ep resin/Un modified AgNbO ₃ nanocomposites		Ep resin/ modified AgNbO ₃ nanocomposites	
Sample wt%	a (kV)	β	a (kV)	β
0	23	18	23	19
1	28	21	33	23
3	26	20	30	18
5	25	19	28	21

Table 5. Weibull parameters for DC flashover strength of ep resin in vacuum incorporated with Un modified and modified AgNbO₂ at different concentrations.

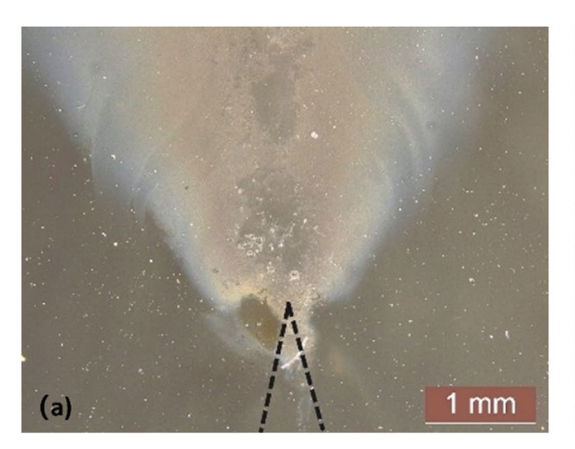




Fig. 12. Surface morphology near the sample needle electrode after pressurization, with dashed lines indicating the needle tip electrode.

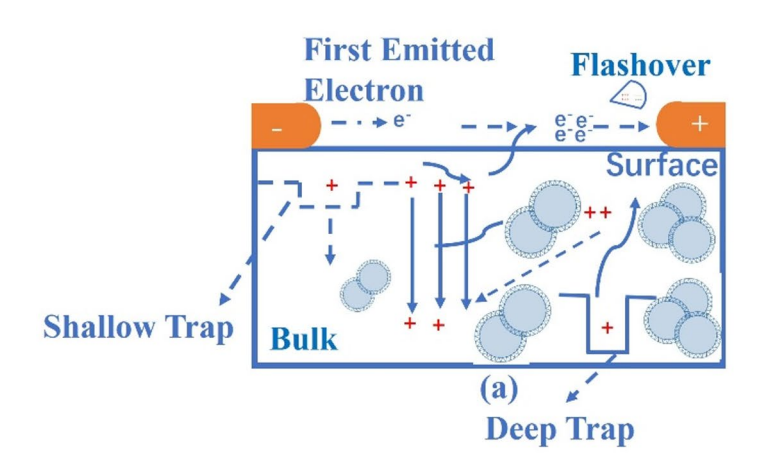
from various angles, resulting in the acceleration of the primary electron by the magnetic field, which is essential for ionization. The gas present on the surface of the dielectric medium simultaneously undergoes desorption or ionization, producing secondary electrons that eventually trigger a secondary electron avalanche. Incorporating $AgNbO_3$ into epoxy resin composites has a notable impact on vacuum flashover behavior and the secondary electron emission characteristics. During the collision ionization phase, some of the generated secondary electrons are captured by traps on the dielectric surface. However, electrical and thermal discharges can rapidly deplete the charge carriers held in shallow traps, thereby reducing their availability. Moreover, the deep traps introduced by $AgNbO_3$ in the epoxy resin can capture electrons that are difficult to release, thereby suppressing electron avalanches and improving the flashover voltage across the vacuum surface. This behavior is closely related to the distribution of surface traps and the resulting influence on surface charge transport properties in epoxy/ Al_2O_3 nanocomposites. Shihu et al. **sexamined how surface trap effects impact flashover voltages in vacuum conditions for epoxy/ Al_2O_3 systems. Both theoretical analysis and experimental findings confirm that the incorporation of an optimal filler concentration significantly enhances surface flashover performance in a vacuum.

Figure 12 shows the surface morphology of epoxy resin before and after modification $AgNbO_3$ nanocomposites after prolonged application of voltage through needle plate electrodes. After being pressurized for 60 min, the epoxy resin incorporated with un modified $AgNbO_3$ at 1 wt% sample showed radial penetrating discharge channels on its surface. There is obvious carbonization marks left that develop clearly in a semi-circular shape towards the surrounding areas. Comparing the development of electric traces in modified $AgNbO_3$ at 1 wt% sample, it can be seen that modified $AgNbO_3$ significantly inhibited the forward development of electric traces. This indicates that after incorporation of modified $AgNbO_3$ not only suppress charge accumulation and also enhanced the flashover field strength.

Discussion

A structural model, shown in Fig. 13, was proposed to evaluate the charge suppression mechanism in $AgNbO_3$ -doped epoxy resin composites before and after surface modification, providing insight into the DC flashover phenomenon. The incorporation of $AgNbO_3$ leads to the formation of both shallow and deep traps. Due to their limited charge retention capacity, shallow traps allow surface charges to escape more readily. At the same time, the modified $AgNbO_3$ particles can influence the surface conductivity of the epoxy resin. This results in a reduction in surface charge accumulation, thereby enhancing the DC flashover strength of the material 46 .

As more AgNbO₃ is added, shallow traps form on the surface, causing a significant increase in surface charges that are involved in discharge processes. However, a significant increase in surface conductivity leads to



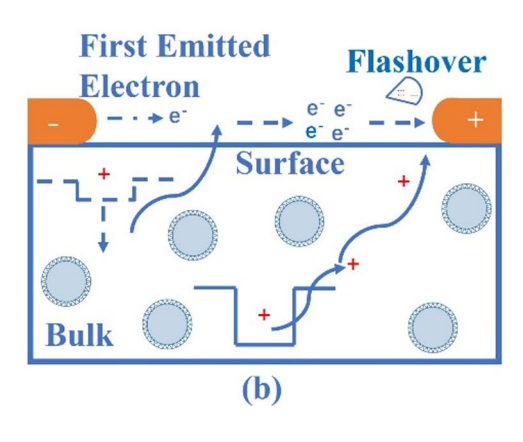


Fig. 13. Schematic diagram of surface flashover of EP resin incorporated with ${\rm AgNbO_3}$ before and after Modification.

a pronounced leakage current at the triple junction where the electrode, epoxy resin, and air converge, resulting in elevated temperatures at that specific interface. In regions with high temperatures, charges migrate swiftly. As a result, surface discharge quickly developed, thereby reducing the intensity of the DC flashover.

Conclusion

This research has conducted a thorough examination of the effects of both unmodified and modified AgNbO₃ particle integration on the electrical properties of Ep resin/AgNbO₃ nanocomposites. The experimental exploration has been conducted on the effects regarding chemical compositions, surface morphology, thermal conductivity, trap levels and DC flashover. The following are the primary conclusions derived from the experimental findings:

- FTIR spectra indicate that the modification of AgNbO₃ particles with the silane coupling agent KH550 has
 resulted in the introduction of organic functional groups on the surfaces. FTIR result being validated using
 XPS. The findings indicate an enhancement in the compatibility and dispersion of AgNbO₃ within the Ep
 resin matrix, as further evidenced by SEM images.
- 2. The incorporation of AgNbO₃ shows a certain enhancement effect in the thermal conductivity of Ep resin. The dielectric permittivity and dielectric loss of Ep resin following the incorporation of modified AgNbO₃ exhibited lower values across all concentrations. This evidence indicates that the silane coupling agent (KH550) acted as an effective barrier between the Ep resin and the modified AgNbO₃, thus restricting the mobility of charge carriers.
- 3. The TSDC measurement reveals that the incorporation of modified AgNbO_3 leads to a change in the trap energy level. The incorporation of a small quantity of AgNbO_3 particles (e.g., 1 wt%) into Ep resin has shown an upward trend in the energy level of deep traps. An improvement of approximately 10% in the DC breakdown strength of Ep resin/AgNbO $_3$ nanocomposites is observed at 1 wt%, following the modification of AgNbO $_3$ with a silane coupling agent.
- 4. The DC flashover measurements indicated that incorporating of modified AgNbO₃ resulted in a noticeable improvement in DC flashover performance in vacuum compared to air. This enhancement is primarily attributed to changes in the trap energy levels of the epoxy resin. The increased trap energy helps suppress secondary electron emission from the epoxy surface. Additionally, adding AgNbO₃ creates deeper traps, which reduces carrier mobility and secondary electron emission, thus suppressing space charge buildup.

Data availability

The datasets used and/or analyzed during the current study available from the corresponding author on reasonable request.

Received: 9 March 2025; Accepted: 25 June 2025

Published online: 02 July 2025

References

- 1. Bhatnagar, N., Ryan, D., Murphy, R. & Enright, A. M. A comprehensive review of green policy, anaerobic digestion of animal manure and chicken litter feedstock potential-Global and Irish perspective, renew. Sust. Energy Rev. 154, 111884 (2022).
- 2. He, A. P., Xue, Q. H., Zhao, R. J. & Wang, D. P. Renewable energy technological innovation, market forces, and carbon emission efficiency. *Sci. Total Environ.* **796**, 148908 (2021).
- 3. Shang, Y., Feng, Y., Zhang, C., Zhang, T. & Chi, Q. Excellent energy storage performance in polymer composites with insulating and polarized two-dimensional fillers. *Comp. Part. A: Appl. Sci. Manu.* 167, 107429 (2023).
- Kitamura, T., Yamada, M., Harada, S. & Koyama, M. Development of High-Power density interleaved dc/dc converter with SiC devices. Electr. Eng. Jpn. 196, 3 (2016).

- 5. Tran, H., Le, T., Jeong, H., Kim, S. J. & Choi, S. W. A 300 khz, 63 kw/l ZVT DC-DC converter for 800-V fuel cell electric vehicles. IEEE Trans. Power Electron. 37, 3 (2022).
- 6. Mengjia, F. et al. Ultrahigh energy storage performance of All-Organic dielectrics at High-Temperature by tuning the density and location of traps mater. *Horizon* 9, 16 (2022).
- 7. Xu, J., Wu, M., Pu, J. & Xue, S. B. Effects of trace oxygen content on microstructure and performances of Au-20Sn/Cu solder joints. Crystal 6, 601 (2021).
- 8. Z.Wang, G. et al. Dielectric and thermal properties characterisation and evaluation of novel epoxy materials for high-voltage power module packaging. *High. Voltage.* **9**, 1021–1032 (2024).
- Chen, S. et al. Enhanced breakdown strength of aligned-sodium-titanate- nanowire/epoxy nanocomposites and their anisotropic dielectric properties. Compos. Part. Appl. Sci. Manuf. 120, 84–94 (2019).
- Ruiyi, L. et al. Review on polymer composites with high thermal conductivity and low dielectric properties for electronic packaging. Mat. Today Phy. 22, 100594 (2022).
- 11. Zhengdong, W. et al. The investigation of the effect of filler sizes in 3D-BN skeletons on thermal conductivity of epoxy-based composite. *Nano-materials* 12, 446 (2022).
- 12. Yalin, W. et al. Space-charge accumulation and its impact on high-voltage power module partial discharge under DC and PWM waves: testing and modeling. *IEEE Trans. Power Electron.* **36** (10), 11097–11108 (2021).
- 13. Dong, W. Z. et al. Boron nitride nanosheet @ quantum-sized diamond nano crystal complex/epoxy nanocomposites with enhancing thermal conductivity and sufficient dielectric breakdown strength. Polym. Com-pos. 45 (4), 3210–3224 (2023).
- 14. Hesham, K., Hanaa, A., Darwish, M. M. F. & Mansour, D. E. The effect of graphene on the thermal and dielectric properties of epoxy resin. In *International Symposium on Electrical Insulating Materials (ISEIM)* 103–106 (2020).
- Zhicheng, W. et al. Computationally driven design of low dielectric-loss epoxy resin for medium-frequency Transformers. J. Phys. Appl. Phys. 18 (56), 184001 (2023).
- 16. Zhang, Y., Wang, H., Huang, Z. & Li, J. Enhanced surface flashover performance of oriented hexagonal Boron nitride composites via anisotropic charge transportation. *High. Voltage.* **9**, 1011–1102 (2024).
- 17. Xie, Q. et al. The synergistic effect of micro structure/nanofiller/super hydrophobicity on the surface flashover. *High. Volt.* 7 (6), 1091–1098 (2022).
- Chi, J., Yuan, R., Zhu, W. & Xing, Y. DC surface flashover of epoxy resin/γ-Al₂O₃ nano-composites for current lead insulation. IEEE Trans. Appl. Super Cond. 31 (8), 1–5 (2021).
- 19. Linker, T. et al. Deep well trapping of hot carriers in a hexagonal Boronnitride coating of polymer dielectrics. ACS Appl. Mater. Interfaces. 13 (50), 60393–60400 (2021).
- Khan, M. Z. et al. Influence of treated Nano-alumina and Gas-phase fluorination on the dielectric properties of epoxy Resin / Alumina nanocomposites. IEEE Trans. Dielectr. Electr. Insul. 27, 410–417 (2020).
- Lingyu, W. et al. Qiang: largely enhanced energy storage density of Poly (vinylidene fluoride) nanocomposites based on surface hydroxylation of Boron nitride nanosheets. J. Mater. Chem. A. 6 (17), 7573–7584 (2018).
- Peixuan, W. et al. Effect of coupling agents on the dielectric properties and energy storage of Ba_{0.5}Sr_{0.5}TiO₃/P(VDF-CTFE) nanocomposites. AIP Adv. 7 (7), 075210 (2017).
- Min, F. et al. Facile synthesis of strontium ferrite nanorods/graphene composites as advanced electrode materials for supercapacitors.
 J. Colloid Interface Sci. 588, 795–803 (2021).
- 24. Hu, P. et al. Topological-structure modulated polymer nanocomposites exhibiting highly enhanced dielectric strength and energy density. *Adv. Funct. Mater.* 24 (21), 3172–3178 (2014).
- Dai, Y. & Zhu, X. Improved dielectric properties and energy density of PVDF composites using PVP engineered BaTiO₃ nanoparticles. Korean J. Chem. Eng. 35 (7), 1570–1576 (2018).
- Zhang, K. et al. DC surface flashover characteristics of ZnO/Epoxy composites at room temperature and 77 K. In IOP Conference Series: Materials Science and Engineering, vol. 756 012004 (IOP Publishing, 2020).
- Lee, Y. J. et al. High voltage dielectric characteristics of epoxy nanocomposites in liquid nitrogen for superconducting equipment. IEEE Trans. Appl. Supercond. 21 (3), 1426–1429 (2010).
- 28. Youping, T. et al. Effect of temperature on polyimide Dc flashover characteristics in different vacuum degrees. *J. Phys. Appl. Phys.* 52 (30), 305201 (2019).
- Wang, Z. et al. Enhancing dielectric properties and energy storage performance of polyvinylidene fluoride composite by surfacemodified AgNbO₃ nanoparticles. High. Voltage. 9, 939–947 (2024).
- 30. Xu, G., Xu, G. & Chang, W. Wang fabrication of microsphere-like nano-MoO2 modified with silane coupling agent KH550. *Mater. Res. Express.* 6 (11), 115087 (2019).
- 31. Ying Wang, Y. et al. Jinhong Yu and Wenge Li epoxy composite with high thermal conductivity by constructing 3D-oriented carbon fiber and BN network structure. RSC Adv. 11, 25422 (2021).
- 32. Zhang, B., Gao, W., Chu, P., Zhang, Z. & Zhang, G. Trap-modulated carrier transport tailors the dielectric properties of alumina/epoxy nanocomposites. *J. Mater. Sci: Mater. Electron.* 29, 1964–1974 (2018).
- 33. Hornak, J. Z. et al. Magnesium oxide nanoparticles: dielectric properties, surface functionalization and improvement of Epoxy-Based composites insulating properties. *Nanomater. (Basel)* 8 (6), 381 (2018).
- Nguyen, T. T. et al. Elaboration and dielectric property of modified pzt/epoxy nanocomposites. Polym. Compos. 37, 455–461 (2016).
- Ramajo, L., Castro, M. S. & Reboredo, M. M. Effect of silane as coupling agent on the dielectric properties of BaTiO₃-epoxy composites. Compos. Part. A. 38, 1852–1859 (2007).
- Chi, J., Yuan, R., Zhu, W. & Xing, Y. DC surface flashover of epoxy Resin/γ-Al₂O₃ nanocomposites for current lead insulation. *IEEE Trans. Appl. Supercond.* 31 (8), 7800205 (2021).
- 37. Xie, Z. et al. Research on electrical properties of surface-modified nano-SiO₂/epoxy composites. In *IEEE International Conference* on High Voltage Engineering and Application (ICHVE) 1–4 (2020).
- 38. Sarathi, R. Understanding the electrical, thermal and mechanical properties of epoxy magnesium oxide nanocomposites. *IET Sci. Meas. Technol.* **13** (5), 632–639 (2019).
- Yun, C. et al. Εροχy/α-alumina nanocomposite with high electrical insulation performance. Progress Nat. Sci.: Mate Inter. 27, 574–581 (2017).
- 40. Turnhout, J. V. In Thermally Stimulated Discharge of Electrets (eds. Electrets) 81-215 (Springer-, 1987).
- Yang, G. et al. Dielectric and relaxation properties of composites of epoxy resin and hyperbranched-polyester-treated Nanosilica. RSC Adv. 8, 30669–30677 (2018).
- 42. Li, S., Yin, G., Bai, S. & Li, J. A new potential barrier model in epoxy resin nanodielectrics. *IEEE Trans. Dielectr. Electr. Insul.* 18, 1535–1543 (2011).
- 43. Cheng, Y., Wang, Z. & Wu, K. Pulsed vacuum surface flashover characteristics of TiO₂/Epoxy Nano-Micro composites. *IEEE Trans. Plasma Sci.* 40, 68–77 (2012).
- 44. Yunqi, W., Bin, W., Jiakai, J. & Peng, H. Study on surface discharge of nonlinear conductive epoxy resin/SrTiO₃ composites in 80–300 K temperature zone. *High. Voltage.* **9** (1), 117–126 (2024).
- 45. Yu, S. et al. Surface trap effects on flashover voltages of epoxy/Al₂O₃ nanocomposites for high voltage insulation. *J. Mat. Sci. Mat. Electro.* **30**, 18135–18143 (2019).

46. Lian, H. et al. Enhancement of surface insulation properties of alumina/epoxy composites through ZrO₂ film sprayed by plasma atomization. *Polym. Compos.* 41, 4020–4030 (2020).

Acknowledgements

This research was funded by the Changzhou Science and Technology Project, Jiangsu, China (Project No. E6-6205-23-038 and Grant No. CQ20234020), and supported by Ongoing Research Funding program, (ORF-2025-646), King Saud University, Riyadh, Saudi Arabia.

Author contributions

Muhammad Zeeshan Khan Methodology, software, draft preparation, sample characterization, investigation, analysis and finalization of experimental setup **Farooq Aslam** Methodology, software, proof reading, formal analysis, journal submission and overall supervision **Faisal Alsaif** Result validation, visualization, draft preparation, revisions and editing.

Competing interests

The authors declare no competing interests.

Additional information

Correspondence and requests for materials should be addressed to M.Z.K. or F.A.

Reprints and permissions information is available at www.nature.com/reprints.

Publisher's note Springer Nature remains neutral with regard to jurisdictional claims in published maps and institutional affiliations.

Open Access This article is licensed under a Creative Commons Attribution-NonCommercial-NoDerivatives 4.0 International License, which permits any non-commercial use, sharing, distribution and reproduction in any medium or format, as long as you give appropriate credit to the original author(s) and the source, provide a link to the Creative Commons licence, and indicate if you modified the licensed material. You do not have permission under this licence to share adapted material derived from this article or parts of it. The images or other third party material in this article are included in the article's Creative Commons licence, unless indicated otherwise in a credit line to the material. If material is not included in the article's Creative Commons licence and your intended use is not permitted by statutory regulation or exceeds the permitted use, you will need to obtain permission directly from the copyright holder. To view a copy of this licence, visit https://creativecommons.org/licenses/by-nc-nd/4.0/.

© The Author(s) 2025